

Increased bone resorption and impaired bone microarchitecture in short-term and extended high-fat diet–induced obesity

Janina M. Patsch^{a,b}, Florian W. Kiefer^c, Peter Varga^d, Pamela Pail^a, Martina Rauner^{a,e}, Daniela Stupphann^a, Heinrich Resch^f, Doris Moser^g, Philippe K. Zysset^d, Thomas M. Stulnig^c, Peter Pietschmann^{a,*}

^a*Division of Cellular and Molecular Pathophysiology, Department of Pathophysiology, Center of Physiology, Pathophysiology and Immunology, Medical University Vienna, A-1090 Vienna, Austria*

^b*Division of Neuroradiology and Musculoskeletal Radiology, Department of Radiology, Medical University Vienna, A-1090 Vienna, Austria*

^c*Clinical Division of Endocrinology and Metabolism, Department of Internal Medicine III, Medical University Vienna, A-1090 Vienna, Austria*

^d*Institute of Lightweight Design and Structural Biomechanics, Vienna University of Technology, A-1040 Vienna, Austria*

^e*Division of Endocrinology, Diabetes, and Bone Diseases, Department of Medicine III, Technical University Dresden, Dresden, Germany*

^f*Medical Department II, St. Vincent Hospital Vienna, A-1060 Vienna, Austria*

^g*Department of Cranio-, Maxillofacial and Oral Surgery, Medical University Vienna, A-1090 Vienna, Austria*

Received 10 October 2008; accepted 17 November 2009

Abstract

Although obesity traditionally has been considered a condition of low risk for osteoporosis, this classic view has recently been questioned. The aim of this study was to assess bone microarchitecture and turnover in a mouse model of high-fat diet–induced obesity. Seven-week-old male C57BL/6J mice ($n = 18$) were randomized into 3 diet groups. One third ($n = 6$) received a low-fat diet for 24 weeks, one third was kept on an extended high-fat diet (eHF), and the remaining was switched from low-fat to high-fat chow 3 weeks before sacrifice (sHF). Serum levels of insulin, leptin, adiponectin, osteocalcin, and cross-linked telopeptides of type I collagen (CTX) were measured. In addition, bone microarchitecture was analyzed by micro-computed tomography; and lumbar spine bone density was assessed by dual-energy x-ray absorptiometry. The CTX, body weight, insulin, and leptin were significantly elevated in obese animals (sHF: +48%, +24%, +265%, and +102%; eHF: +43%, +52%, +761%, and +292%). The CTX, body weight, insulin, and leptin showed a negative correlation with bone density and bone volume. Interestingly, short-term high-fat chow caused similar bone loss as extended high-fat feeding. Bone volume was decreased by 12% in sHF and 19% in eHF. Bone mineral density was 25% (sHF) and 27% (eHF) lower when compared with control mice on low-fat diet. As assessed by the structure model index, bone microarchitecture changed from plate- to rod-like appearance upon high-fat challenge. Trabecular and cortical thickness remained unaffected. Short-term and extended high-fat diet–induced obesity caused significant bone loss in male C57BL/6J mice mainly because of resorptive changes in trabecular architecture.

© 2011 Elsevier Inc. All rights reserved.

1. Introduction

Obesity affects more than 300 million adults worldwide, and its prevalence is predicted to rise over the next decades [1]. Osteoporosis, a skeletal disorder characterized by compromised bone strength, is considered of similar socioeconomic importance [2]. Osteoporosis causes a significant increase in fracture risk [3]. Health care costs related to osteoporotic

fractures currently produce expenses greater than \$17 billion in the United States and are projected to rise by more than one third by 2025 [4]. Low body mass index (BMI) is an established risk factor for bone loss [5]. Traditionally, obesity has been believed to protect the skeleton; and a great number of studies have reported a positive relation between bone density and BMI [6]. Nevertheless, this formerly clear association is increasingly being questioned. Despite the fact that obesity is on a constant rise in the United States, analyses comparing the prevalence of osteoporosis in National Health and Nutrition Examination Survey III with National Health and Nutrition Examination Survey 1999–2002 could not detect a general

* Corresponding author. Tel.: +43 1 40400 5126; fax: +43 1 40400 3031.

E-mail address: peter.pietschmann@meduniwien.ac.at (P. Pietschmann).

“antiosteoporotic” trend [7]. Especially in men, lean body mass was repeatedly shown to be a stronger determinant of bone mineral density (BMD) than mere BMI [8,9]. Upon correction of bone density measurements for the mechanical loading effects of increased body weight, fat mass was shown to inversely correlate with bone mass [10]. Several animal studies support the negative impact of overweight and “Western” diets on bone health [11,12]. However, neither the pattern nor the mechanism of obesity-associated bone disease has been studied in detail up to now. Some studies focusing on atherogenic, high-fat diet suggest an acquired defect in osteoblast differentiation and function [13,14]. In light of the common lineage of osteoblasts and adipocytes, a large body of evidence supports a close and tightly regulated cellular interplay of fat and bone [15]. The role of osteoclasts (the bone resorbing cells) is largely unknown in terms of obesity. C57BL/6J is a mouse strain prone to diet-induced obesity, age-related osteoporosis, and general susceptibility to bone loss [16–18]. With a mouse model for high-fat diet-induced obesity at hand, the aim of the present study was to dissect the biological details of diet-induced obesity-associated bone loss after short-term and extended high-fat feeding.

2. Methods

2.1. Animals

C57BL/6J mice were purchased from Charles River Laboratories (Sulzfeld, Germany) and maintained at the Institute of Biomedical Research, Medical University Vienna, Austria. Food and water were provided ad libitum, and all mice were kept on a 12-hour light/12-hour dark cycle. At the age of 7 weeks, 18 male animals were randomized into 3 groups: low-fat diet for 24 weeks (LF, $n = 6$), short-term high-fat chow (sHF, $n = 6$), and extended high-fat chow for 24 weeks (eHF, $n = 6$). The sHF group received low-fat chow for 21 weeks and was then switched to high-fat chow for 3 weeks. In the low-fat control group, 10% of total calories were based on lipids, whereas high-fat feeding exposed the animals to 60% lipids. All animal diets were purchased from Research Diets, New Brunswick, NJ. After intraperitoneal anesthesia, a retroorbital blood sample was collected at the age of 31 weeks. Finally, the mice were killed by cervical dislocation. The animal study protocol was approved by the ethical committee for animal experiments of the Medical University Vienna. We certify that all applicable institutional and governmental regulations concerning ethical use of animals were followed during this research.

2.2. Laboratory measurements

Commercially available enzyme-linked immunosorbent assay kits were used to determine fasting plasma insulin (Mercodia, Uppsala, Sweden), C-reactive protein (CRP; Alpco Diagnostics, Salem, NH), leptin (R and D Systems, Minneapolis, MN), adiponectin (adipoQ; Alpco Diagnos-

tics), and cross-linked telopeptides of type I collagen (CTX) (Rat Laps; Nordic Bioscience, Herlev, Denmark). Fasting plasma osteocalcin concentrations were measured using an indirect immunoradiometric assay (Immutopics, San Clemente, CA).

2.3. Dual-energy x-ray absorptiometry

Vertebral columns were dissected and placed in 70% ethanol. Dual-energy x-ray absorptiometry (DXA) measurements of lumbar spines were carried out on a conventional DXA scanner (iDXA; GE Lunar, Madison, WI). Software initially designed for scanning human hands (Encore 11.20, GE Lunar), was applied to visualize and measure the samples. For each sample, a 1.5-cm-long, user-defined region of interest was set 1 mm cranially the lumbosacral junction. The pattern of software-based bone recognition was checked and adapted manually when required.

2.4. Micro-computed tomography

Lumbar spines were further dissected into separate vertebrae. The posterior parts were removed to achieve optimal alignment in the sample holder and to facilitate the contouring process. In each mouse, the fourth lumbar vertebra (L4) was scanned. The vertebrae were scanned in a 70% alcohol solution at an isotropic spatial resolution of 12 μm ($\mu\text{CT}40$; Scanco Medical, Bruetisellen, Switzerland). Settings for the scanning protocol were 70 peak kilovolt, 114 mA, and 200-millisecond integration time. The computed tomographic (CT) images were filtered with a Gaussian filter ($\sigma = 0.8$, support = 1) and segmented with an individual threshold value for each sample that was computed with an adaptive-iterative algorithm as the local minimum between the 2 peaks in the actual gray scale histogram. Regions of the endplates were excluded from the analysis, and the cortical and trabecular phases were identified and separated using an automated procedure implemented in IPL (Image Processing Language, Scanco Medical, Bruetisellen, Switzerland) [19,20]. The latter required the definition of the vertebral contour that was drawn with a semiautomated method. Model-independent 3-dimensional morphologic indices of the trabecular compartment were evaluated using the standard procedures of the software. Results of the direct (ie, voxel based) measurements were used for further analysis [21,22]. Cortical thickness was measured with the distance-transform method [21].

2.5. Static histomorphometry

After removal of L4 for micro-CT (μCT), the remaining undecalcified vertebral columns were embedded in polymethylmethacrylate for histologic analysis (Technovit 9100; Heraeus Kulzer, Wehrheim, Germany). Two-micrometer-thick sections were cut and Goldner stained; and for each sample, the third lumbar vertebra was analyzed in a semiquantitative manner using standard histomorphometry software (Osteomeasure; Osteometrics, Decatur, GA).

Table 1
Metabolic data and laboratory measurements

	LF	sHF	eHF
Body weight (g)	33.4 ± 1.0	41.3 ± 1.6*	50.8 ± 0.8* [†]
GWAT weight (g)	1.16 ± 0.1	1.93 ± 0.2*	1.66 ± 0.04*
Insulin (μU/mL)	5.4 ± 1.3	19.7 ± 4.3*	46.5 ± 14.0* [†]
Leptin (ng/mL)	19.8 ± 3.0	39.9 ± 7.8	77.5 ± 8.0* [†]
Adiponectin (μg/mL)	54.6 ± 2.3	58.8 ± 3.7	71.1 ± 6.5*
CRP (ng/mL)	105.0 ± 3.2	94.5 ± 10.6	118.6 ± 2.6 [†]
IL-6 (pg/mL)	3.1 ± 0.9	3.9 ± 1.1	3.7 ± 0.4
CTX (ng/mL)	23.2 ± 2.4	34.3 ± 2.1*	33.2 ± 2.2*
Osteocalcin	57.8 ± 2.9	ND	55.1 ± 4.4

All values are given as means ± SEM. IL-6 indicates interleukin-6; ND, not determined.

* Different from LF ($P < .05$).

[†] Different from sHF ($P < .05$).

2.6. Statistical analysis

All statistical analyses were performed on SPSS 13 (Version 13.0.0; SPSS, Chicago, IL) for Mac OS X. Because of skewed data, the Wilcoxon rank sum test was applied to detect statistically significant differences. The level of significance was set at $P < .05$. Because of the small sample size, we did not perform multiplicity corrections to avoid an increasing error of the second type. Correlations were expressed by Spearman coefficient.

3. Results

3.1. Weight, fasting plasma insulin, and bone metabolism

According to nutritional fat content and the duration of high-fat feeding, the highest body weight was detected in eHF mice. Differences in body weight were significant

between every single feeding group. Gonadal white adipose tissue (GWAT) mass was significantly elevated in sHF and eHF compared with LF, but there was no difference between the 2 high-fat groups (Table 1). Insulin plasma levels were increased 3.6- and 8.6-fold in sHF and eHF, respectively. Leptin was raised 2-fold in sHF and 3.9-fold in eHF. However, adiponectin was highest in eHF. When compared with LF controls, the bone resorption parameter (CTX) was significantly elevated with high-fat feeding (sHF: +47.8%, eHF: +43.1%). Bone formation, as assessed by osteocalcin plasma levels, did not differ between eHF and controls. The highest CRP plasma levels were exhibited in eHF, whereas there was no significant difference between LF and sHF. Interleukin-6 plasma levels were unaltered in the 3 study groups (Table 1).

3.2. Bone quality

Bone mineral density as assessed by DXA indicated a substantial bone loss of 24.6% in sHF and 27.3% in eHF mice when compared with LF. Bone mineral density of sHF and eHF did not differ significantly (Fig. 1D). Using μ CT, these results were confirmed by a significant and proportionate decrease of 11.7% (sHF) and 19.1% (eHF) in bone volume (BV/TV). Different from DXA, μ CT yielded a significant difference in BV/TV between eHF and sHF (Fig. 1E). A mineralization disorder (ie, increased osteoid surface) was excluded by static histomorphometry. The amount of bone surface covered by osteoblasts (Ob.S/BS) or osteoclasts (Oc.S/BS) was similar in all 3 groups (data not shown). In parallel to a significant increase in trabecular separation (Fig. 2C), the number of trabeculae was reduced in eHF mice (Fig. 2A). Trabecular thickness remained

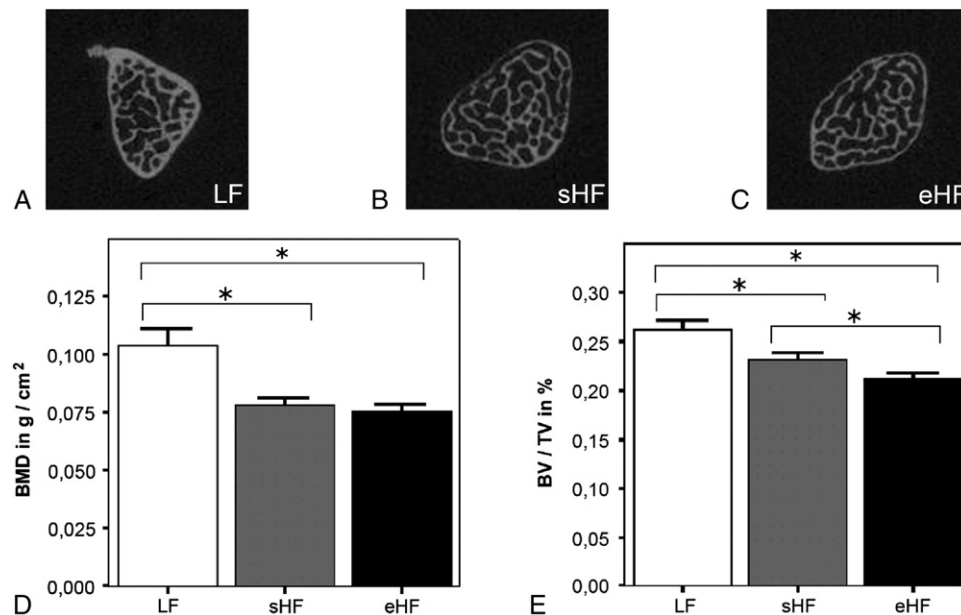


Fig. 1. Micro-computed tomography and DXA. The μ CT-based cross section of fourth lumbar vertebral body representative per group (A–C), bone density as assessed by DXA (D), and bone volume as assessed by μ CT (E). The asterisk (*) indicates a P value $< .05$.

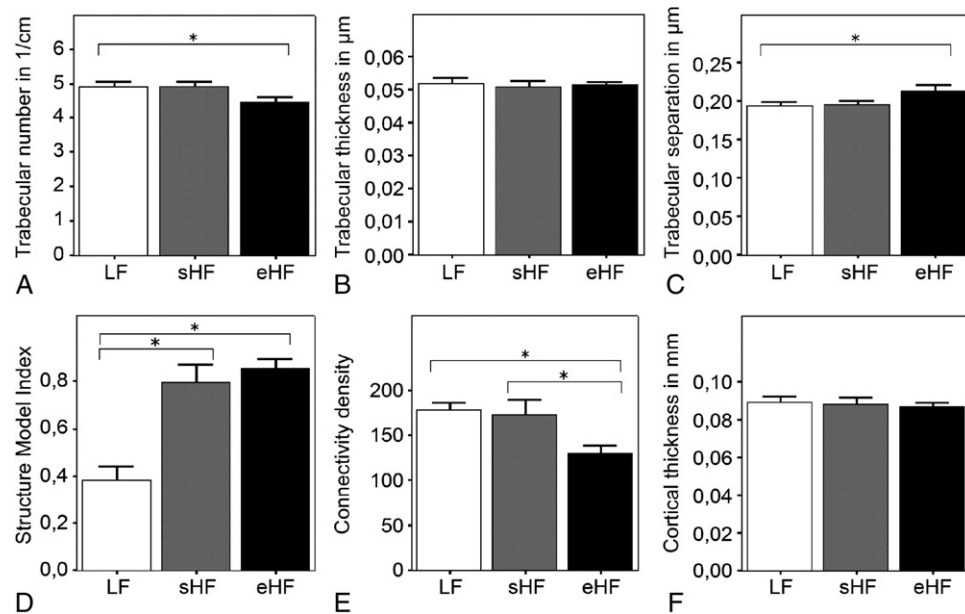


Fig. 2. Bone microarchitecture. All parameters are μ CT derived. The asterisk (*) indicates a P value < .05.

unchanged (Fig. 2B), but connectivity density was significantly decreased in eHF when compared with both other groups (Fig. 2E). Followed by sHF mice, eHF animals displayed the highest structure model index (SMI, Fig. 2D). Interestingly, cortical thickness remained unaffected by diet-induced weight gain (Fig. 2F).

3.3. Correlation analyses

Body weight correlated significantly with insulin and leptin plasma levels. The degree of hyperinsulinemia correlated negatively with BMD, BV/TV, trabecular number, and connectivity density. Similar to body weight, GWAT, insulin, and leptin, the resorption marker CTX was associated

with increases in SMI. Moreover, increased body weight was significantly correlated with deleterious changes in bone quality, that is, bone density, bone volume, connectivity density, trabecular number, and trabecular separation. Leptin was inversely associated with connectivity density and further displayed a moderate negative correlation with BMD and BV/TV. All correlation details are presented in Table 2.

4. Discussion

Despite the formerly widespread belief in mutual exclusiveness of obesity and osteoporosis, a certain association of overweight and decreased bone mass has

Table 2
Correlations independent of groups (Spearman coefficient)

	BMD	Weight	GWAT	Insulin	Leptin	Adipo	CTX	OCN	IL-6	CRP	BV/TV	Ct Th	Conn	SMI	TbN	TbTh	TbSp
Weight	-0.60																
GWAT	-0.39	0.53															
Insulin	-0.50	0.83	0.55														
Leptin	-0.57	0.81	0.34	0.67													
Adipo	-0.33	0.60	0.49	0.62	0.35												
CTX	-0.53	0.42	0.29	0.60	0.22	0.40											
OCN	0.19	-0.15	0.11	-0.10	-0.15	-0.10	-0.28										
IL-6	-0.01	0.04	0.04	0.14	-0.23	0.21	0.13	0.11									
CRP	-0.19	0.71	0.15	0.56	0.58	0.66	0.06	-0.05	-0.22								
BV/TV	0.63	-0.79	-0.33	-0.62	-0.57	-0.41	-0.38	0.34	0.03	-0.47							
Ct Th	0.26	0.05	0.36	0.00	-0.17	0.21	0.17	-0.49	0.09	-0.13	-0.02						
Conn	0.35	-0.82	-0.43	-0.69	-0.65	-0.46	-0.22	0.48	-0.02	-0.68	0.68	-0.17					
SMI	-0.60	0.66	0.54	0.64	0.54	0.45	0.48	-0.26	0.18	0.19	-0.80	0.18	-0.42				
TbN	0.23	-0.68	-0.19	-0.50	-0.45	-0.42	-0.14	0.51	0.14	-0.73	0.79	-0.11	0.83	-0.45			
TbTh	0.33	0.02	0.21	0.04	0.03	0.10	-0.14	-0.08	0.04	0.21	0.27	0.32	-0.35	-0.22	-0.11		
TbSp	-0.15	0.58	0.13	0.39	0.34	0.32	0.05	-0.57	-0.22	0.66	-0.75	0.13	-0.77	0.37	-0.98	0.08	

Significant correlations are printed in bold ($P < .05$). Adipo indicates adiponectin; OCN, osteocalcin; Ct Th, cortical thickness; Conn, connectivity density; TbN, trabecular number; TbTh, trabecular thickness; TbSp, trabecular separation.

been described in humans and laboratory animals. A cross-sectional study examining body composition, hip density, and geometry in community-dwelling men revealed a negative relation of fat mass, BMI, and proximal femoral bone strength [23]. Extreme obesity was also shown to impair bone density in both ovariectomized mice and postmenopausal women [24]. However, pathogenetic mechanisms and the process of bone loss as such have not yet been further elucidated.

Being part of the metabolic syndrome, insulin resistance is tightly interwoven with obesity [25]. At the time they were killed, our animals were clearly obese. Short-term and extended high-fat diet–fed mice had significantly higher GWAT weight compared with LF controls (Table 1). Gonadal white adipose tissue, seen as the most metabolic active adipose tissue in mice, corresponds to the visceral adipose tissue in humans [26] and correlates with body weight and insulin in our study. In our experimental groups, an increase in fasting plasma insulin was observed along with an increase in body weight (Table 1). Insulin per se acts as an osteoanabolic agent *in vivo* and *in vitro* [27,28]. Nevertheless, lower bone density and increased fracture risk are seen in patients with type 2 diabetes mellitus [29–31]. In our study, insulin levels were negatively correlated with bone volume (BV/TV); and hyperinsulinemia was associated with increased bone resorption (Table 2). Obese, hyperinsulinemic mice displayed high leptin. Leptin and adiponectin are heavily influenced by obesity and interfere with bone metabolism in a complex manner [32,33]. Leptin was shown to influence bone metabolism negatively via a hypothalamic pathway. Mediated by the sympathetic nerve system, leptin exerts an inhibitory function to osteoblasts [34]. Osteoblasts, which share the mesenchymal lineage with adipocytes, are increasingly considered as endocrine cells. They seem to be able to regulate energy metabolism via a classic feedback loop: Stressing the cross talk of bone and energy metabolism, osteocalcin (an osteoblast-specific protein) stimulates insulin and adiponectin release [35]. Accordingly, osteocalcin-deficient mice are insulin resistant [36]. In our study, osteocalcin remained unchanged upon high-fat diet; but leptin was correlated negatively with BMD, BV/TV, and connectivity density. Interestingly, adiponectin displayed parallel increases with leptin and was high in obese animals (Tables 1 and 2). Although adiponectin was reported to preserve bone both *in vivo* and *in vitro* [37], we were unable to find any relation to bone turnover or bone quality. Both adipokines were positively correlated with the inflammation marker CRP (Table 2). Increased CRP was repeatedly shown to be related to low bone quality and osteoporotic fractures [38,39]. Accordingly, cancellous bone was lower in connectivity and trabecular number with increasing CRP levels (Table 2).

Uncontrolled bone resorption is a major cause of a fast decrease in bone mass both in men and laboratory animals [40–44]. In our study, the bone resorption marker CTX was significantly elevated in both groups of obese mice (Table 1).

As indicated by similar CTX levels in sHF and eHF, the degree of bone resorption was comparable among both obese groups. Interestingly, vertebral bone volume loss in sHF was almost as pronounced as in eHF, indicating only a limited dependence on obesity duration (Fig. 1). Moreover, changes in the SMI were detectable in both groups of obese animals. The SMI describes if an examined volume of trabecular bone has either plate- or rod-like properties and is thus a suitable tool to describe subtle ongoing changes in bone microarchitecture. The values for mammalian spongiosa range from 0 to 3, with 0 being the ideal plate and 3 the ideal rod [22]. In our study, significantly increased SMI values mice indicate the presence of more rod-like spongiosa in both groups of obese animals. Moreover, body weight and leptin were positively correlated with the SMI in all groups. Interestingly, trabecular thickness remained unaffected overall. This unexpected finding is best explained by considering the computation of the parameter itself: simplified, trabecular thickness is calculated as the most frequently occurring diameter of a virtual ball fitting into trabecular structures [21]. Applied to a single arbitrary trabecular plate, the SMI's chronological advance in displaying microarchitectural changes can be explained by observing that, even if a plate turns into a rod, local trabecular thickness remains unchanged unless the minimal diameter of the rod falls below the minimal diameter of the plate (Fig. 3). Conformingly, the standard deviation of trabecular thickness decreases with higher body weight. Considering the obesity-duration-dependent decrease of trabecular number and separation in eHF but not sHF (Fig. 2), longer high-fat exposition than in that explored in this study could also affect trabecular thickness.

When compared with other studies inducing experimental bone loss in male mice (eg, using orchidectomy), the speed and extent of trabecular bone loss due to diet-induced obesity were lower [45]. Human *in vitro* data suggest decreased osteoclast generation in the presence of leptin [46]. Given the equal osteoclast surfaces in lean and obese animals, we conclude that in our mouse model, osteoclasts are not numerically augmented but seem to be in a hyperactive state.

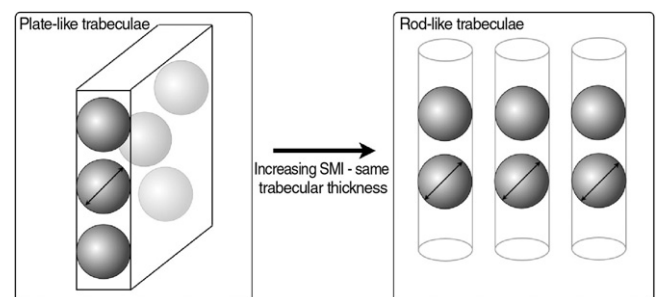


Fig. 3. Explanatory scheme for plate-to-rod transformation without decrease in trabecular thickness. Measurement of trabecular thickness is based on the most frequent diameter of a virtual ball fitting into trabecular structures. Plate-to-rod changes are captured by increases in the SMI. In our animal model, trabecular thickness still remained unchanged.

Although not tested in this study, alterations in the equilibrium of the receptor activator of nuclear factor κ B ligand and its endogenous opponent osteoprotegerin could be of pivotal importance in obesity-associated osteoclast activation [47].

Interpreting the bone formation marker osteocalcin and the bone resorption marker CTX together, bone resorption markedly prevailed over bone formation. Obesity and type 2 diabetes mellitus were both shown to be negatively associated with parameters of bone formation, indicating a potential acquired osteoblast defect [48,49]. In our study, plasma osteocalcin levels were unaltered despite elevated CTX. We therefore speculate about a potential osteoblast-osteoclast coupling defect in high-fat diet-induced obesity (Table 1).

Summarizing our experiments, we were able to demonstrate increased bone resorption after short-term and extended high-fat feeding in male C57/BL/6J mice. As a consequence, bone density and bone microarchitecture are significantly impaired in both obesity-inducing diet regimens. Stressing the complex, dynamic character of bone resorption as a biological process, trabecular connectivity loss and plate-to-rod transformations seem to co-occur in high-fat diet-induced obesity.

Acknowledgment

This research was supported by the Austrian Science Fund project # P 20239-B13 (to P.P.), the Austrian Science Fund project no. P18776-B11 and as part of CCHD (W1205-B09), and the European Community's 7th Framework Programme (FP7/2007-2013) under grant agreement no. 201608 (all to T.M.S.).

The authors are grateful to Katharina Wahl, Ines Fischer, and Michael Weber for technical support.

References

- [1] Haslam DW, James WP. Obesity. *Lancet* 2005;366:1197-209.
- [2] Cole ZA, Dennison EM, Cooper C. Osteoporosis epidemiology update. *Curr Rheumatol Rep* 2008;10:92-6.
- [3] Kanis JA, Borgstrom F, De Laet C, et al. Assessment of fracture risk. *Osteoporos Int* 2005;16:581-9.
- [4] Burge R, Dawson-Hughes B, Solomon DH, et al. Incidence and economic burden of osteoporosis-related fractures in the United States, 2005-2025. *J Bone Miner Res* 2007;22:465-75.
- [5] Kanis JA. Diagnosis of osteoporosis and assessment of fracture risk. *Lancet* 2002;359:1929-36.
- [6] Felson DT, Zhang Y, Hannan MT, et al. Effects of weight and body mass index on bone mineral density in men and women: the Framingham study. *J Bone Miner Res* 1993;8:567-73.
- [7] Looker AC, Flegal KM, Melton 3rd LJ. Impact of increased overweight on the projected prevalence of osteoporosis in older women. *Osteoporos Int* 2007;18:307-13.
- [8] Reid IR, Plank LD, Evans MC. Fat mass is an important determinant of whole body bone density in premenopausal women but not in men. *J Clin Endocrinol Metab* 1992;75:779-82.
- [9] Barondess DA, Nelson DA, Schlaen SE. Whole body bone, fat, and lean mass in black and white men. *J Bone Miner Res* 1997;12:967-71.
- [10] Zhao LJ, Liu YJ, Liu PY, et al. Relationship of obesity with osteoporosis. *J Clin Endocrinol Metab* 2007;92:1640-6.
- [11] Zernicke RF, Salem GJ, Barnard RJ, et al. Long-term, high-fat-sucrose diet alters rat femoral neck and vertebral morphology, bone mineral content, and mechanical properties. *Bone* 1995;16:25-31.
- [12] Demigné C, Bloch-Faure M, Picard N, et al. Mice chronically fed a westernized experimental diet as a model of obesity, metabolic syndrome and osteoporosis. *Eur J Nutr* 2006;45:298-306.
- [13] Parhami F, Jackson SM, Tintut Y, et al. Atherogenic diet and minimally oxidized low density lipoprotein inhibit osteogenic and promote adipogenic differentiation of marrow stromal cells. *J Bone Miner Res* 1999;14:2067-78.
- [14] Parhami F, Tintut Y, Beamer WG, et al. Atherogenic high-fat diet reduces bone mineralization in mice. *J Bone Miner Res* 2001;16:182-8.
- [15] Rosen CJ, Buxsein ML. Mechanisms of disease: is osteoporosis the obesity of bone? *Nat Clin Pract Rheumatol* 2006;2:35-43.
- [16] Beamer WG, Donahue LR, Rosen CJ, et al. Genetic variability in adult bone density among inbred strains of mice. *Bone* 1996;18:397-403.
- [17] Buxsein ML, Myers KS, Shultz KL, et al. Ovariectomy-induced bone loss varies among inbred strains of mice. *J Bone Miner Res* 2005;20:1085-92.
- [18] Collins S, Martin TL, Surwit RS, et al. Genetic vulnerability to diet-induced obesity in the C57BL/6J mouse: physiological and molecular characteristics. *Physiol Behav* 2004;81:243-8.
- [19] Buie HR, Campbell GM, Klinck RJ, et al. Automatic segmentation of cortical and trabecular compartments based on a dual threshold technique for in vivo micro-CT bone analysis. *Bone* 2007;41:505-15.
- [20] Lublinsky S, Ozcivici E, Judex S. An automated algorithm to detect the trabecular-cortical bone interface in micro-computed tomographic images. *Calcif Tissue Int* 2007;81:285-93.
- [21] Hildebrand T, Rüegsegger P. A new method for the model independent assessment of thickness in three-dimensional images. *J Microsc* 1997;185:67-75.
- [22] Hildebrand T, Rüegsegger P. Quantification of bone microarchitecture with the structure model index. *Comput Methods Biomech Biomed Engin* 1997;1:15-23.
- [23] Travison TG, Araujo AB, Esche GR, et al. Lean mass and not fat mass is associated with male proximal femur strength. *J Bone Miner Res* 2008;23:189-98.
- [24] Núñez NP, Carpenter CL, Perkins SN, et al. Extreme obesity reduces bone mineral density: complementary evidence from mice and women. *Obesity (Silver Spring)* 2007;15:1980-7.
- [25] Selwyn AP. Weight reduction and cardiovascular and metabolic disease prevention: clinical trial update. *Am J Cardiol* 2007;100:33-7.
- [26] Guerre-Millo M. Adipose tissue hormones. *J Endocrinol Invest* 2002;25:855-61.
- [27] Yano H, Ohya K, Amagasa T. Effects of insulin on in vitro bone formation in fetal rat parietal bone. *Endocr J* 1994;41:293-300.
- [28] Thrallkill KM, Lumpkin Jr CK, Bunn RC, et al. Is insulin an anabolic agent in bone? Dissecting the diabetic bone for clues. *Am J Physiol Endocrinol Metab* 2005;289:E735-745.
- [29] Kinjo M, Setoguchi S, Solomon DH. Bone mineral density in adults with the metabolic syndrome: analysis in a population-based U.S. sample. *J Clin Endocrinol Metab* 2007;92:4161-4.
- [30] Ahmed LA, Schirmer H, Berntsen GK, et al. Features of the metabolic syndrome and the risk of non-vertebral fractures: the Tromsø study. *Osteoporos Int* 2006;17:426-32.
- [31] Hofbauer LC, Brueck CC, Singh SK, et al. Osteoporosis in patients with diabetes mellitus. *J Bone Miner Res* 2007;22:1317-28.
- [32] Thomas T, Burguera B. Is leptin the link between fat and bone mass? *J Bone Miner Res* 2002;17:1563-9.
- [33] Oh KW, Lee WY, Rhee EJ, et al. The relationship between serum resistin, leptin, adiponectin, ghrelin levels and bone mineral density in middle-aged men. *Clin Endocrinol (Oxf)* 2005;63:131-8.
- [34] Ducky P, Amling M, Takeda S, et al. Leptin inhibits bone formation through a hypothalamic relay: a central control of bone mass. *Cell* 2000;100:197-207.

- [35] Confavreux CB, Levine RL, Karsenty G. A paradigm of integrative physiology, the crosstalk between bone and energy metabolisms. *Mol Cell Endocrinol* 2009 [Epub ahead of print].
- [36] Lee NK, Sowa H, Hinoi E, et al. Endocrine regulation of energy metabolism by the skeleton. *Cell* 2007;130:456–69.
- [37] Williams GA, Wang Y, Callon KE, et al. In vitro and in vivo effects of adiponectin on bone. *Endocrinology* 2009 [Epub ahead of print].
- [38] Schett G, Kiechl S, Weger S, et al. High-sensitivity C-reactive protein and risk of nontraumatic fractures in the Bruneck study. *Arch Intern Med* 2006;166:2495–501.
- [39] Ding C, Parameswaran V, Udayan R, et al. Circulating levels of inflammatory markers predict change in bone mineral density and resorption in older adults: a longitudinal study. *J Clin Endocrinol Metab* 2008;93:1952–8.
- [40] Lloyd SA, Yuan YY, Kostenuik PJ, et al. Soluble RANKL induces high bone turnover and decreases bone volume, density, and strength in mice. *Calcif Tissue Int* 2008;82:361–72.
- [41] Mundy GR. Osteoporosis and inflammation. *Nutr Rev* 2007;65: S147–51.
- [42] Gorai I, Taguchi Y, Chaki O, et al. Specific changes of urinary excretion of cross-linked N-telopeptides of type I collagen in pre- and postmenopausal women: correlation with other markers of bone turnover. *Calcif Tissue Int* 1997;60:317–22.
- [43] Erben RG, Eberle J, Stahr K, et al. Androgen deficiency induces high turnover osteopenia in aged male rats: a sequential histomorphometric study. *J Bone Miner Res* 2000;15:1085–98.
- [44] Most W, van der Wee-Pals L, Ederveen A, et al. Ovariectomy and orchidectomy induce a transient increase in the osteoclastogenic potential of bone marrow cells in the mouse. *Bone* 1997;20:27–30.
- [45] Venken K, De Gendt K, Boonen S, et al. Relative impact of androgen and estrogen receptor activation in the effects of androgens on trabecular and cortical bone in growing male mice: a study in the androgen receptor knockout mouse model. *J Bone Miner Res* 2006;21:576–85.
- [46] Holloway WR, Collier FM, Aitken CJ, et al. Leptin inhibits osteoclast generation. *J Bone Miner Res* 2002;17:200–9.
- [47] Kong YY, Yoshida H, Sarosi I, et al. OPGL is a key regulator of osteoclastogenesis, lymphocyte development and lymph-node organogenesis. *Nature* 1999;397:315–23.
- [48] Holecki M, Zahorska-Markiewicz B, Janowska J, et al. The influence of weight loss on serum osteoprotegerin concentration in obese perimenopausal women. *Obesity (Silver Spring)* 2007;15:1925–9.
- [49] Pietschmann P, Scherthaner G, Woloszczuk W. Serum osteocalcin levels in diabetes mellitus: analysis of the type of diabetes and microvascular complications. *Diabetologia* 1988;31:892–5.